Research Article

A Computational Analysis of the Soret and Dufour Effects on a Rotating Hybrid Nanofluid

Alfunsa Prathiba*[1] , Venkata A. Lakshmi[2] and V. Ramesh[2]

[1] *Department of Mathematics, CVR College of Engineering, Hyderabad, India*
[2] *Department of Mathematics, Osmania University, Hyderabad, India*
*Corresponding author: alphonsaperli@gmail.com

Abstract. This paper shows the impact of the Dufour and Soret numbers on a *hybrid nanofluid* (HNF) in a boundary layer area across a spinning sheet. The collection of flow governing (PDEs) partial differential equations was turned into a system of (ODEs) ordinary differential equations, which are then solved utilising BVP4C code in MATLAB. The impact of the flow governing parameters on the flow properties were analysed and presented graphically. The Soret factor influences the thermal efficiency at the surface, while the Dufour effect reduces the mass transfer at the surface.

Keywords. Hybrid nanofluid, Rotating sheet, Lobatto III A technique, Soret, Dufour

Mathematics Subject Classification (2020). 76A05, 76A10, 76Dxx, 76R10, 76R50, 76Uxx

1. Introduction

Research is being done on the enhancement of the thermal conductivity in various materials owing to the demand in heat transfer applications. Choi and Eastman [10] used nanoparticles for the first time by incorporating a thin suspension of nano particles suspension into the liquid base. The nanofluids are widely employed in heat exchangers, nuclear reactors, microelectronics, bio-medicine, and many more (Khan [31]). To investigate thermal energy flow in nanofluids, Buongiorno [9] has created a two-piece relationship based on two major slip characters, namely "Brownian motion, and thermophoresis". Nayak *et al.* [30] in their study, investigated the MHD nanofluids flow by connecting it with porous matrix and Patel model that provided a

significant development in the heat transfer capabilities of the nano fluid. Ali *et al.* [2], gave the experimental findings of water based ZnO nanoparticles to alter the heat changes for a car's radiator. Arshad and Ali [5] experimentally investigated the characteristics of heat transfer and pressure fall of Titanium nanoparticles through a mini-channel and explained that the thermal behaviour of TiO_2 had strong impact on the heating capacity. Further, Saffarian *et al.* [40] have used nanofluid to modify a solar collector's heat transfer (HETR) across a flat surface via several pathways. Recently, Rana *et al.* [36] in their investigation examined the 3-D steady flow of an incompressible 25 nm water based Cu nano liquid over a bi-directional extended surface, also Corcione's model for dynamic viscosity and effective thermal boundary conductivity was utilised in conjunction with specific heat, electric conductivity connexions constructed on effective medium theory.

Despite varied utilitarian benefits some nanofluids have been identified as hybrid or second-grade fluids due to their advanced rheological capabilities and thermo-physical properties. These fluids are formed from two distinct nano-material suspensions in a base liquid. Various researchers have explored this innovative class of heat transmission fluids to identify answers to real-world issues and it has been widely used in many domains, such as biomedicine, drug delivery, cooling of machines and many more. Waini *et al.* [50] in their analysis discovered that only one solution was stable among the dual solutions of the dusty HNF in an existing magnetic field, along a shrinking sheet. Lund *et al.* [25] in their investigation studied the rotating 3-D flow of a HNF over an exponential sheet with suction effects and found that a symmetrical solution existed for changes in rotation parameter. Kumar *et al.* [22] estimated the Natural convection 3D hydro magnetic flow and heat transfer of hybrid nanoparticles and hybrid nanoparticles generated in Carreau hybrid base fluid consisting of the activations of thermal shapes nanoparticles using R-K Fehlberg method. Many researchers have recently explored the heat transfer trend in hybrid nano flow. A remarkable amount of research has been conducted on the production, categorization and applications of various varieties of hybrid nano fluids [1, 3, 6, 11–13, 23, 38, 45].

Great deal of research is done on the flow of fluids and heat conduction phenomenon in revolving frames. It is due to their abundant utilitarian benefits in computer storage devices, crystal growth, gas turbine propellers etc. Aziz *et al.* [7], in their investigation of an optimal study for 3D rotating flow of Oldroyd-B nanofluid fluid with convectively heated surface, and had noticed a substantial rise in temperature for improved values of Prandtl and Biot number. Kumar *et al.* [21] have investigated the flow of Se anoparticles over a rotating exponential sheet due to solar radiation and found that the rise in temperature and thermal layer thickness was due to the existence of solar radiation. Furthermore, Turkyilmazoglu [48] explored the flow and heat transfer of an incompressible electrically conducting fluid over a rotating infinite disk, using the Optimal homotopy technique. Hayat *et al.* [17]., studied thermophysical characteristics of Cu-water nano tube with engine and kerosine oils in rotating porous disk using Darcy-Forcheimer medium. Khan *et al.* [16] gave the comparison of heat transfer properties of MHD rotating nanofluid with that of emerging hybrid nanofluid. Khan *et al.* [20], have analysed

the thermophysical traits of MHD Williamson fluid under the influence of Joule heating and activation energy over a rotating sheet and observed that higher values of thermal conductivity, Eckert number and solar radiation parameters the temperature profile increases, on the other hand opposite behaviour is noticed for Prandtl number. Mustafa *et al.* [29], recently used Cattaneo-Christov heat flux theory to find the analytical solutions of 3-D rotating floes of Old Royd-B liquid.

The driving potential is more complex when heat and mass transfer phenomena occur simultaneously among the fluxes as energy flux can be created not only by temperature gradients but also by composition gradients [50]. The Dufour or diffusion thermo effect is the energy flux generated by composition gradient. Correspondingly, the Soret is triggered by a temperature gradient, causing mass fluxes. The effects exhibited by Fick's or Fourier laws are of higher order than the Soret and Dufour effects [41]. Charles Soret, a Swiss chemist, was the first to use the thermo-diffusion effect to investigate the gravity of Earth in detail in 1879. Soret also noticed that a salt solution in a tube with two ends at different temperatures did not remain uniform in composition, and salt was concentrated more towards the colder end than the heated end of the tube [50]. Shaheen *et al.* [44] in their investigation explored the effects of variable characteristics on a 3-D dusty Casson fluid flow past a deformable bidirectional surface amalgamated with Arrhenius activation energy and chemical reaction. Rasool *et al.* [37], studied "the consequences of binary chemical reaction, thermal radiation, and Soret-Dufour effects on a steady incompressible Darcy-Forchheimer flow of nanofluids". Further, numerous investigations on the effects of Soret and Dufour were performed by various researchers using numerical and analytical methods on a variety of fluid flows [35, 39, 43, 47].

Shoaib *et al.* [46] investigated the flow properties of HNF over a rotational disk subjected to Joule heating implementing the Lobatto IIIA technique. Arif *et al.* [19] utilised FEM along with the Lobatto III-A to investigate the dispersion of both single and combined nanoparticles in a fluid under the influence of the magnetic field with viscosity and on a non-uniform surface. Ouyang *et al.* [32] has learned about, the radiative flow of an MHD hybrid nanofluid (Al_2O_3- Cu/H_2O) over a convectively heated stretchable rotating disc with velocity slip effects was numerically treated using the Lobatto IIIA technique. Uddin [49] explored the capability of a numerical computational structure based on the Lobatto IIIA approach for the *Darcy-Forchheimer* flow of *Sisko* nanomaterials with nonlinear thermal radiation.

As witnessed in the above-mentioned works and due to their large potential industrial applications, the Soret and Dufour effects have become a prominent field of study. Thus, our goal is to explore numerically theses effects on the HNF flow over a revolving sheet through this article. Through similarity transformation, the boundary layered PDEs of the physical flow were turned into ODEs and an efficient mathematical tool BVP4C code in MATLAB was implemented to solve them. The correctness of the code was ensured by comparative study of previous works as a limiting condition.

2. Mathematical Formulation

Consider the 3D flow of Al_2O_3-Cu/water nano particles across a $z = 0$ plane as the stretchy surface. The chosen hybrid nano particles and the base liquids are assumed to be in "thermal equilibrium". The fluid is capturing the half space at $z \geq 0$. As seen in Figure 1, the surface extends in the x-direction with a linearly varying velocity $U_w = ax$, causing flow in adjacent liquid layers. Let Ω be the rotating liquid's constant angular velocity. The surface temperature T_w and T_∞ the ambient temperature of the hybrid nanofluid is constant. The concentration of the hybrid nanofluid is given by C_w.
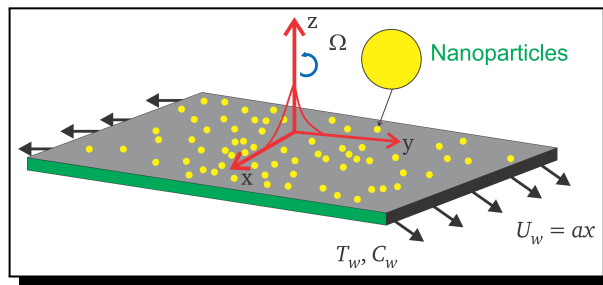
Figure 1. Physical model of the problem

After applying the boundary layer approximations, the governing equations for the hybrid nanofluid can be stated as follows [4, 31, 42, 50, 52].

The continuity equation,

$$u_x + v_y + w_z = 0. \tag{2.1}$$

The momentum equations

$$uu_x + vu_y + wu_z = \frac{\mu_{hnf}}{\rho_{hnf}}u_{zz} + 2\Omega v, \tag{2.2}$$

$$uv_x + vv_y + wv_z = \frac{\mu_{hnf}}{\rho_{hnf}}v_{zz} - 2\Omega u. \tag{2.3}$$

The energy equation

$$uT_x + vT_y + wT_z = \frac{k_{hnf}}{(\rho C_p)_{hnf}}T_{zz} - \frac{1}{(\rho C_p)_{hnf}}q_{rz} + \frac{D_M k_T}{C_s(\rho C_p)_{hnf}}C_{zz}. \tag{2.4}$$

The equation of concentration

$$uC_x + vC_y + wC_z = D_{hnf}C_{zz} + \frac{D_M k_T}{T_M}T_{zz}. \tag{2.5}$$

The boundary restrictions are,

$$u = U_w\lambda, \ v = 0, \ w = w_w, \ T = T_w, \ C = C_w \text{ at } z = 0,$$

$$u \to 0, \ v \to 0, \ T \to T_\infty, \ C \to C_\infty \text{ as } z \to \infty. \tag{2.6}$$

In equations (2.1)-(2.6), u, v, w are the velocity components of the hybrid nanofluid along the x, y, z-direction. T, q_r, C are the temperature, radiative heat flux (Gireesha *et al*. [14]) and concentration of the hybrid nanofluid respectively. λ is the stretching parameter (Anuar *et al*. [4]). Further D_M, D_{hnf} is the "mass diffusivity coefficient", the thermal diffusion

ratio is given by K_T, and the mean fluid temperature and the concentration susceptibility are given by T_M and C_s, respectively.

The thermophysical properties of the hybrid nanofluid such as dynamic viscosity, thermal conductivity etc are given in Table 2. Further the physical relations of the hybrid nanofluid used in the above equations are stated in Table 1.

Table 1. Thermophysical relations of the fluid [15, 28, 46]

Properties	Hybrid nanofluid
Density, ρ	$\frac{\rho_{hnf}}{\rho_f} = \left[\left(\frac{\rho_{s1}}{\rho_f}\right)\phi_1 + (1-\phi_1)\right](1-\phi_2) + \phi_2\frac{\rho_{s2}}{\rho_f}$
Heat capacity, ρC_p	$[\rho C_p]_{hnf} = [\rho C_p]_f\left[\left(\frac{(\rho C_p)_{s1}}{(C_p\rho)_f}\right)\phi_1 + (1-\phi_1)(1-\phi_2) + \phi_2(\rho C_p)_{s2}\right]$
Dynamic viscosity, μ	$\frac{\mu_{hnf}}{\mu_f} = \frac{1}{[(1-\varphi_1)(1-\varphi_2)]^{5/2}}$
Thermal conductivity [32], k	$\frac{k_{hnf}}{k_{bf}} = \frac{k_{s2}+k_{bf}(s-1)-(k_{bf}-k_{s2})(s-1)\varphi_2}{k_{bf}(s-1)+(k_{bf}-k_{s2})\varphi_2+k_{s2}}$ and $\frac{k_{bf}}{k_f} = \frac{k_{s1}+k_f(s-1)-(k_f-k_{s1})(s-1)\varphi_1}{k_f(s-1)+(k_f-k_{s1})\varphi_2+k_{s1}}$

Here, hnf, bf, f, $s1$, $s2$ are the subscripts which are related to HNF, base fluid, solid nano particle1 (Al_2O_3), "solid or fluid nano particle2 (Cu)". The volume fraction of the nanoparticle alumina and Copper are given by ϕ_1 and ϕ_2, to get the desired combination of the hybrid nanofluid alumina is introduced into the base fluid (water) and then the copper particles and $\varphi_1 = 0.01$ is the constant volume fraction taken throughout the analysis. The radiation term q_r which can be expressed according to the Rosseland approximation [4], [26] can be given as below,

$$q_r = -\frac{4\sigma_0}{3k^*}\frac{\partial T^4}{\partial z},$$

where σ_0 and k^* are the Stefan-Boltzmann constant and the coefficient of mean absorption, respectively [4]. Ignoring the higher order terms and using the Taylor series, T^4 is expanded about T_∞; hence we get $T^4 \approx 4T_\infty^3 T - 3T_\infty^4$, then equation (2.4) can be rewritten as

$$uT_x + vT_y + wT_z = \frac{k_{hnf}}{(\rho C_p)_{hnf}}T_{zz} + \frac{16\sigma_0 T_\infty^3}{3k^*(\rho C_p)_{hnf}}T_{zz} + \frac{D_M k_T}{C_s(\rho C_p)_{hnf}}C_{zz}. \tag{2.7}$$

The following similarity transformations [4], [27] have been utilised in this problem to modify the PDE to ODE

$$u = axf'(\eta), \ v = axg(\eta), \ w = -\sqrt{a\vartheta_f}f(\eta), \ \theta(\eta) = \frac{T-T_\infty}{T_w-T_\infty}, \ \Phi(\eta) = \frac{C-C_\infty}{C_w-C_\infty}, \ \eta = z\sqrt{\frac{a}{\vartheta_f}}. \tag{2.8}$$

The differentiation with respect to η is indicated by prime and $w_w = -\sqrt{a\vartheta_f}S$, in which a is a constant and S is the mass flux parameter. If $S > 0$ corresponds to suction and $S < 0$ relates to injection. Equation (2.1) identically verified and equations (2.2), (2.3), (2.7) and (2.5) are changed to ODE's as listed below,

$$\frac{\mu_{hnf}/\mu_f}{\rho_{hnf}/\rho_f}f''' + ff'' - (f')^2 + 2\omega g = 0, \tag{2.9}$$

$$\frac{\mu_{hnf}/\mu_f}{\rho_{hnf}/\rho_f}g'' - f'g + fg' - 2\omega f' = 0, \tag{2.10}$$

$$\frac{(\rho C_p)_f}{(\rho C_p)_{hnf}} \left\{ \frac{1}{\Pr} \left[\frac{k_{hnf}}{k_f} + \frac{4}{3} R_d \right] \theta'' + Du\Phi'' \right\} + f\theta' = 0, \tag{2.11}$$

$$\Phi'' + \frac{D_f}{D_{hnf}} Sc[f\Phi' + Sr\theta''] = 0, \tag{2.12}$$

subject to

$$f'(\eta) = \lambda, \ g(\eta) = 0, \ f(0) = S, \ \theta(\eta) = 1, \ \Phi(\eta) = 1, \ \text{as } \eta \to 0,$$

$$f'(\eta) \to 0, \ g(\eta) \to 0, \ f(0) \to 0, \ \theta(\eta) \to 0, \ \Phi(\eta) \to 0, \ \text{as } \eta \to \infty. \tag{2.13}$$

In equations (2.9)-(2.12) the non-dimensional parameters present are given as

$$\omega = \frac{\Omega}{a}, \ \Pr = \frac{\vartheta_f(\rho C_p)_f}{k_f}, \ Sc = \frac{\vartheta_f}{D_f}, \ R_d = \frac{4\sigma_0 T_\infty^3}{k^* k_f}, \ Du = \frac{D_M K_T}{Cs(\rho C_p)_f \vartheta_f} \left[\frac{C_w - C_\infty}{T_w - T_\infty} \right],$$

$$Sr = \frac{D_M K_T}{T_M \vartheta_f} \left[\frac{T_w - T_\infty}{C_w - C_\infty} \right].$$

The Skin friction coefficients C_{fx} and C_{fy} along the axis x and y, as well as the local Nusselt number Nu_x and the local Sherwood number Sh_x are stated as below ([34]),

$$C_{fx} = \frac{\mu_{hnf}}{\rho_f U_w^2} \left(\frac{\partial u}{\partial z} \right)_{z=0}, \ C_{fy} = \frac{\mu_{hnf}}{\rho_f U_w^2} \left(\frac{\partial v}{\partial z} \right)_{z=0},$$

$$Nu_x = \frac{x}{k_f(T_w - T_\infty)} \left[-k_{hnf} \left(\frac{\partial T}{\partial z} \right)_{z=0} + q_r \Big|_{z=0} \right], \ Sh_x = \frac{x}{D_f(T_w - T_\infty)} \left[-D_{hnf} \left(\frac{\partial C}{\partial z} \right)_{z=0} \right] \tag{2.14}$$

From equations (2.8) and (2.14) the modified values of the above as

$$Re_x^{1/2} C_{fx} = \frac{\mu_{hnf}}{\mu_f} f''(0), \ Re_x^{1/2} C_{fy} = \frac{\mu_{hnf}}{\mu_f} g'(0),$$

$$Re_x^{-1/2} Nu_x = -\left(\frac{k_{hnf}}{k_f} + \frac{4R_d}{3} \right) \theta'(0), \ Re_x^{-1/2} Sh_x = -\left(\frac{D_{hnf}}{D_f} \right) \Phi'(0). \tag{2.15}$$

Table 2. The thermophysical properties [4, 24, 33]

Properties	Base fluid	Nano particles	
	Water	Al$_2$O$_3$ (Alumina)	Cu (Copper)
Thermal conductivity (k)(Wm^{-1}K^{-1})	0.613	40	400
Density (ρ) (kgm^{-3})	997.1	3970	8933
Specific heat (Cp)(Jkg^{-1}K^{-1})	4179	765	385

3. Method of Solution

Lobatto IIIA is integrated into MATLAB routine "BVP4C" was implemented to solve the equations (2.9) to (2.12) along the boundary conditions (2.13). In this method $h = 0.01$ was used as the step size and the procedure is continued until the results are accurate to the desired level of precision 10^{-6}. Figure 2 depicts the solution strategy for the problem.

The parameters A_1, A_2, A_3, B_1, B_2 are stated below as,

$$A_1 = \frac{\mu_f}{\mu_{hnf}}, \ A_2 = \frac{\rho_{hnf}}{\rho_f}, \ A_3 = \frac{(\rho C_p)_{hnf}}{(\rho C_p)_f}, \ B_1 = \frac{k_{hnf}}{k_f} + \frac{4}{3} R_d, \ B_2 = \frac{1}{(1-\phi_1)(1-\phi_2)}.$$
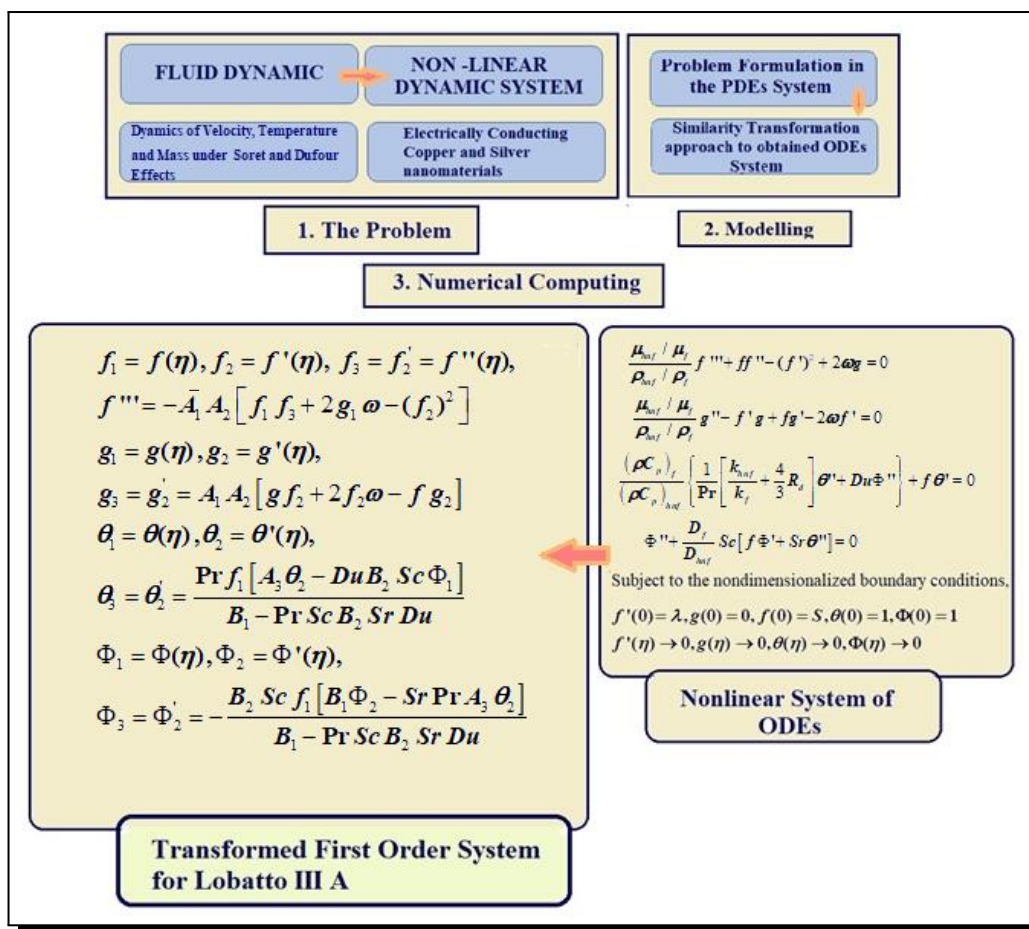
Figure 2. Graphical abstract of the problem

4. Results and Discussion

The numerical solution for the modified ODEs under various parameter values are displayed in Figures 3-19. The description of the behaviour of velocity, concentration, and temperature of an Al_2O_3-Cu-water based flow across a revolving sheet has been presented in detail. The results, as shown in Table 3 and Table 4 were compared and determined to be in good agreement to give the authenticity of the code.

In this segment, the effects of various significant parameters such as nano-particle volume fraction (ϕ_2), Dufour (Du), Soret (Sr), rotation parameter (ω), radiation parameter (R_d), Suction parameter (S), and Schmidt parameter (Sc) on the flow parameters are described.

Higher rotational parameter values produce lower velocity distributions since the rotational parameter is the ratio of rotation to stretching rates in physical terms'. In Figure 3, the impact of the rotation parameter (ω) on the non-dimensional velocities in the x-direction was observed and found that the higher values of the rotation parameter result in a faster rotational rate, which corresponds to a decrease in the velocity distribution $f'(\eta)$. Figure 4 reveals that the rise in the values of ω decays the velocity distribution $g(\eta)$. It is so because the rotational parameter is crucial in accelerating the flow along y-direction and the more significant rotational parameter produces an oscillating pattern in the velocity distribution.

Table 3. Comparison of the values of $f''(0)$, $g'(0)$, $Re_x^{-1/2}Nu_x$ for base fluid when $\varphi_1 = \varphi_2 = 0$, $Du = Sr = Sc = 0$ and $\lambda = 1$

	Wang [51]		Bachok *et al.* [8]			Present study		
ω	$f''(0)$	$g'(0)$	$f''(0)$	$g'(0)$	$Re_x^{-0.5}Nu_x$	$f''(0)$	$g'(0)$	$Re_x^{-0.5}Nu_x$
0.00	-1.00000	0.00000	-1.00000	0.00000	14.78568	-1.0000	0.000000	14.7857
0.50	-1.1384	-0.5128	-1.13838	-0.51276	14.78408	-1.1384	0.5128213	14.7841
1.00	-1.3250	-0.8371	-1.32503	-0.83710	14.78039	-1.3250	0.8371426	14.7804
2.00	-1.6523	-1.2873	-1.6524	-1.28726	17.775800	-1.6524	1.287323	17.7758

Table 4. Comparison of the values of $Re_x^{-1/2}Sh_x$ for base fluid when $\varphi_1 = 0.1$, $Du = Sr = Sc = 0$ and $\lambda = 1$ for different values of φ_2

| φ_2	λ	Du	Sr	Waini *et al.* [50]	Present study
0	0	0	0	0.5739	0.573879
0.02				0.5734	0.573396
0.04				0.5724	0.572384
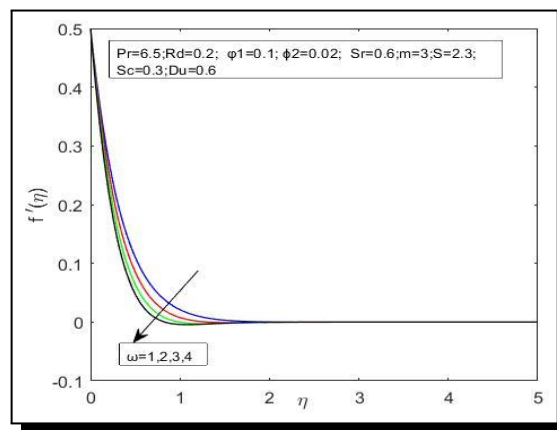
**Figure 3.** Behaviour of $f'(\eta)$ with ω
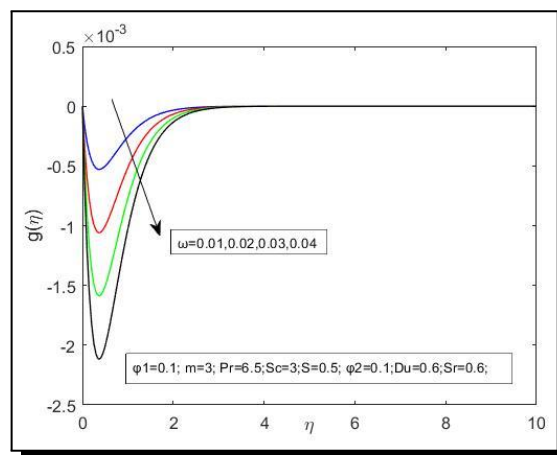
Figure 4. The impact of the rotational parameter (ω) on $g(\eta)$

The impact of the radiation parameter (Rd) on the temperature and concentration distribution was presented in Figure 5 and Figure 6. With the rise in the values of the thermal radiation parameter, the temperature and concentration boundary layers increase. Consequently, the boundary layers grow with the increased thermal radiation. As a result, it has been suggested that the lowering of thermal radiation must proceed at a faster diffusion rate.
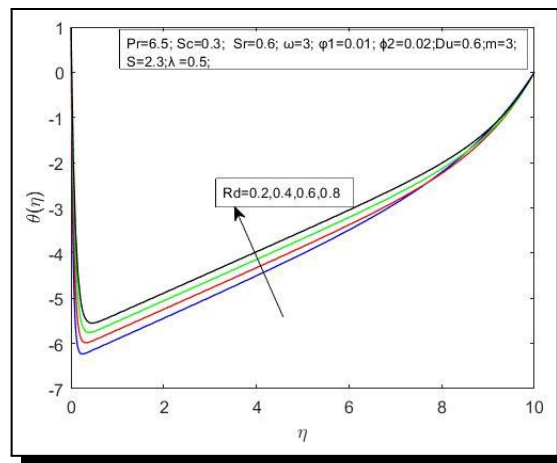

Figure 5. Impact of Rd on the temperature profile
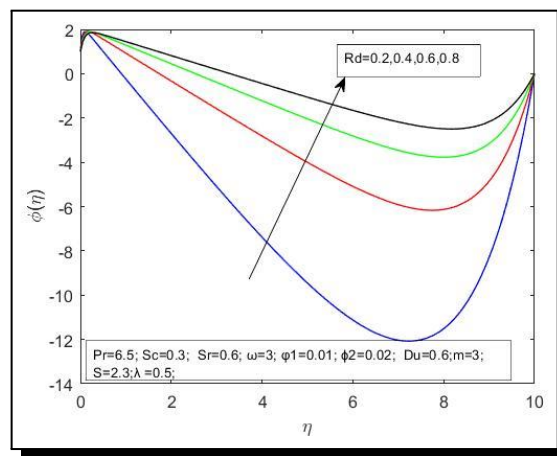
Figure 6. The impact on radiation parameter (Rd) on the concentration profile

Figure 7 to Figure 10 show the influence of the mass flux parameter S, i.e., the suction parameter, on the non-dimensional distribution of velocity, temperature, and concentration. The plots reveal that velocity rate in x-direction decreases significantly with an increase in suction parameter ($S > 1$) whereas the reverse effect is observed in the velocity in the *y-direction*. And it is noted that the increase in the values of suction parameter decrease the temperature and diffusion of the nanofluid.

Figure 11 and Figure 12 were plotted to examine the influence of the *Soret* (Sr) and the *Dufour* (Du) on the concentration and temperature boundary layers, respectively. From the diagrams, we observe the significant decline in nanoparticle concentration profiles for higher
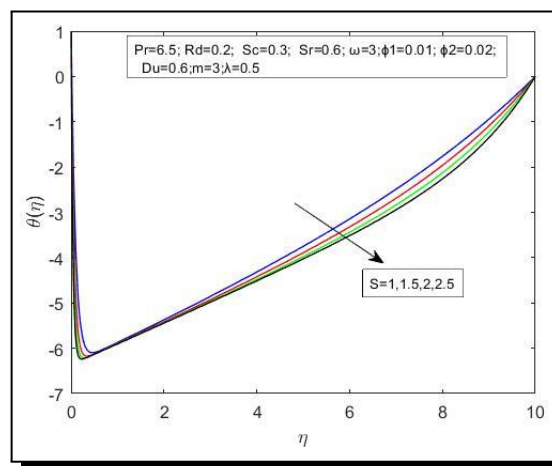
values of the Sr, under the influence of suction ($S > 1$). The reduction in concentration is associated with the thermophoresis effect. Similarly, we observed that the rise in Du values decrease the temperature profiles.
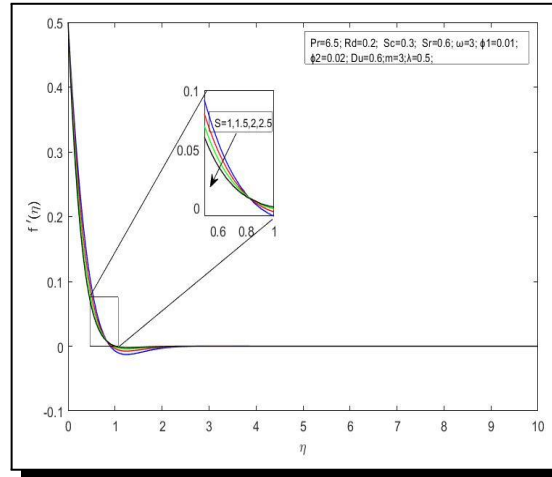
Figure 7. Changes in $f'(\eta)$ for different values of S
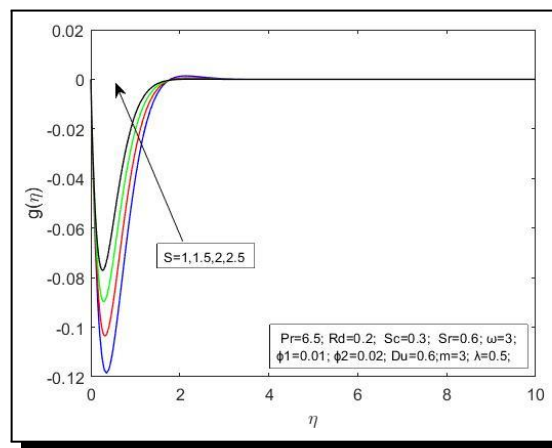
Figure 8. The surge in transverse velocity for S

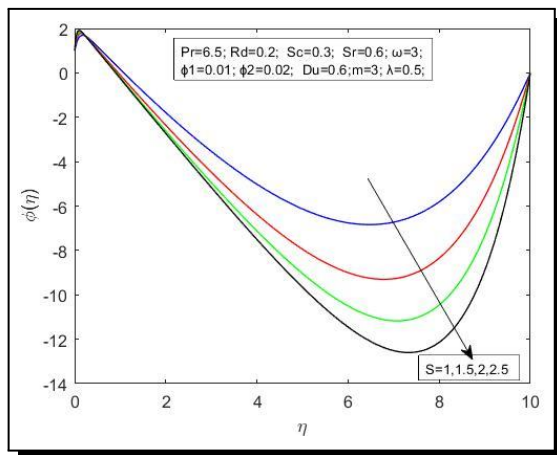**Figure 9.** Influence of S on $\theta(\eta)$

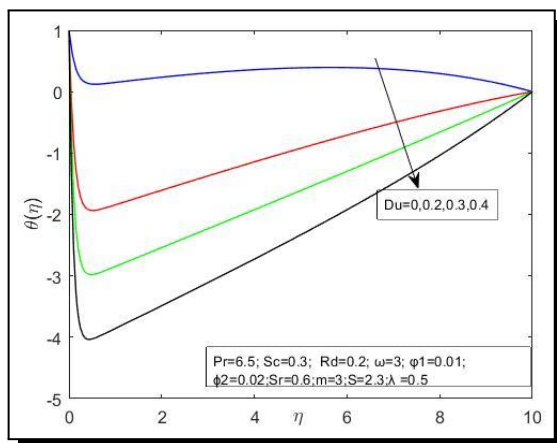**Figure 10.** Impact of suction on $\Phi(\eta)$

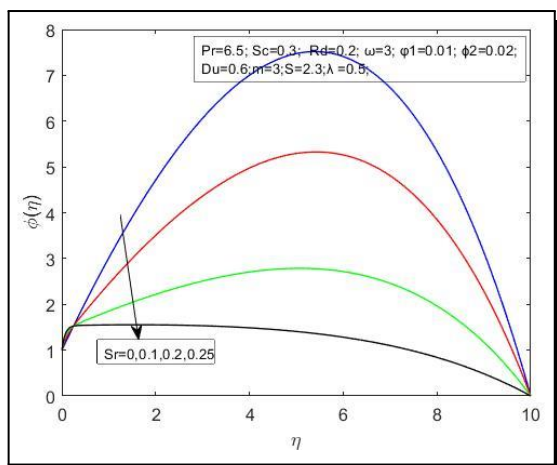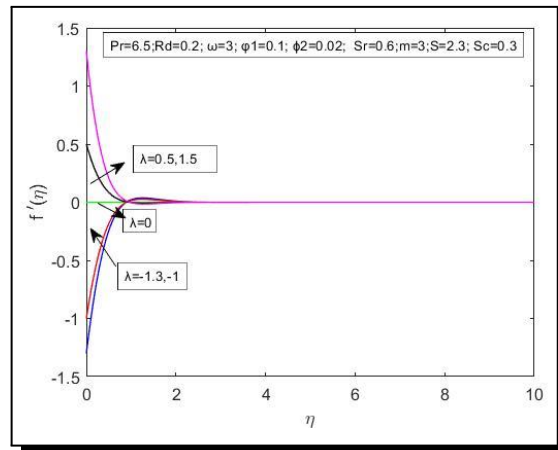**Figure 11.** Impact of Du on $\theta(\eta)$

Figure 12. Impact of Soret on concentration

Figure 13 and Figure 14 display the influential variation of the stretching parameter λ on the velocity boundary layer and it reveals that the greater values of the stretching parameter constitute a higher velocity distribution and vice-versa for $f'(\eta)$. The converse effects are observed on $g(\eta)$.
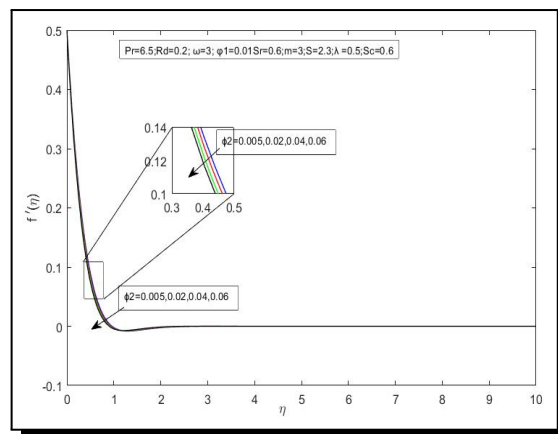
Figure 13. Influence of λ on $f'(\eta)$
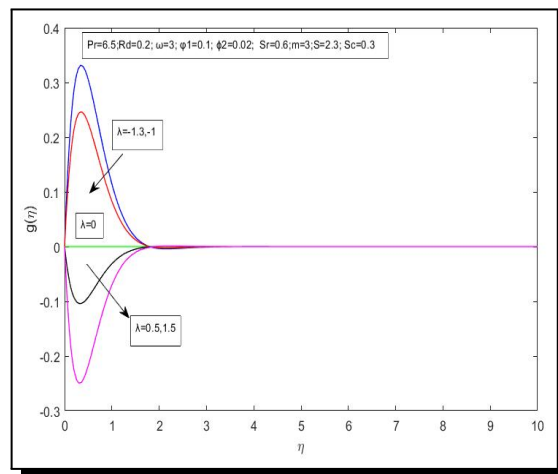
Figure 14. Impact of stretching parameter λ on $g(\eta)$

The influence of variation in the nanoparticle volume fraction $\phi_2(0.005, 0.02, 0.04, 0.06)$ of the Cu (Copper) in the water-based Al_2O_3 nanofluid can be visualized from the plots (Figure 15 to Figure 18). They show that the rise in the concentration values of Cu enhances the profile $g(\eta)$, $\Phi(\eta)$ and reduces the profiles of $f'(\eta)$ and $\theta(\eta)$.

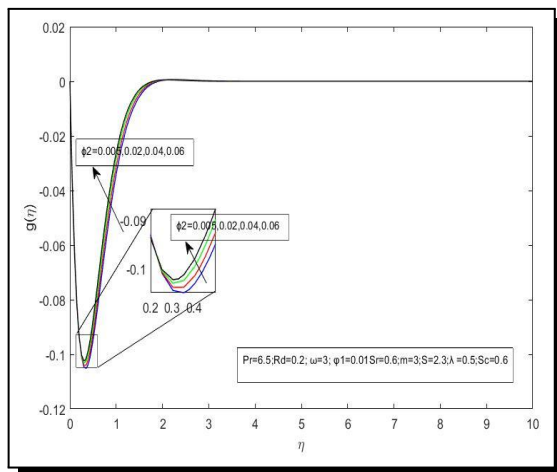**Figure 15.** The variation in primary velocity with ϕ_2

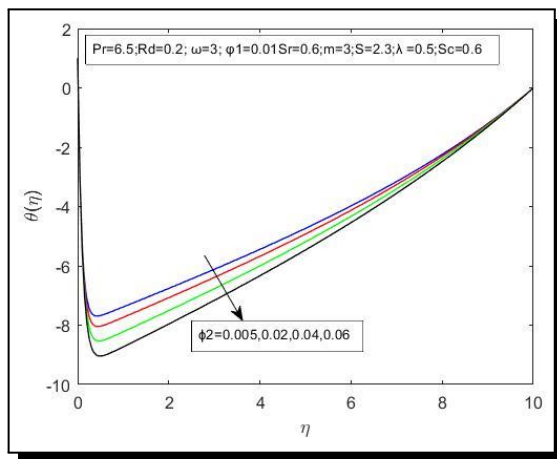**Figure 16.** The transverse velocity profile variations with ϕ_2

Figure 17. Influence of ϕ_2 on the temperature profile
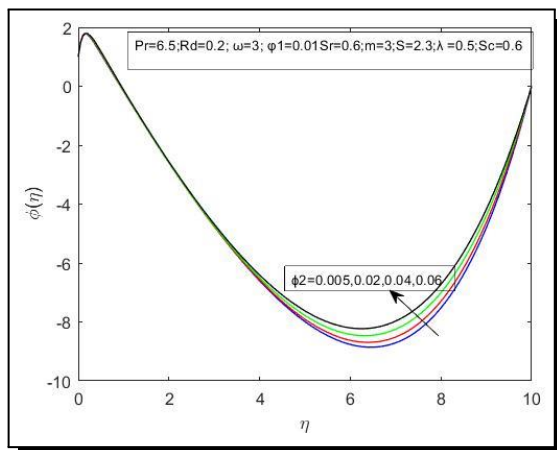

Figure 18. Impact of ϕ_2 on the concentration

For the increased values of the Schmidt parameter, it is anticipated from the plot that there is a decline in concentration profiles (Figure 19). It is so because the Schmidt number is defined as the ratio of momentum to mass diffusivities. Hence the rise in Sc values is responsible for reducing concentration profiles.
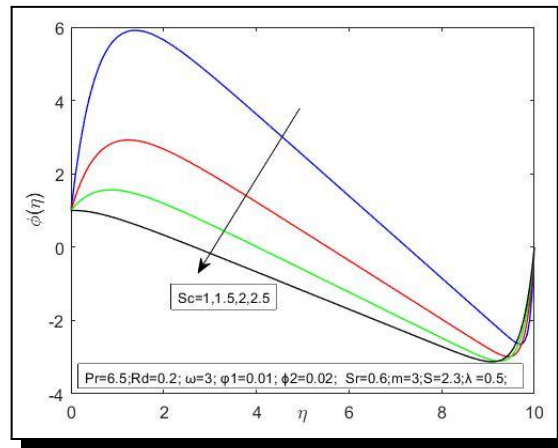
Figure 19. Impact of S on the concentration profile

Table 5 illustrates the computational values of the Nusselt Number, Mass diffusion coefficient (Sh_x), local Skin friction values for distinct values of Soret, Dufour, the nanoparticle volume fraction of Cu, suction etc. From the above table, we observe that the $Re_x^{-1/2}Nu_x$, $-Re_x^{-1/2}Sh_x$ values shoot up with the enhancement in Sr, Du, ϕ_2, S, and decline with rise in the values of R_d. The local skin friction C_{fx} increase with increase in the values of ϕ_2, S, whereas C_{fy} tends to exhibit the variant behaviour for the various values of suction and volume fraction parameters.

Table 5. Computational values of $Re_x^{1/2}C_{fx}$, $Re_x^{1/2}C_{fy}$, $Re_x^{-1/2}Nu_x$, $Re_x^{-1/2}Sh_x$ for various values of Sr, Du, ϕ_2, S, R_d

Sr	Du	ϕ_2	S	R_d	$-Re_x^{1/2}C_{fx}$	$-Re_x^{1/2}C_{fy}$	$Re_x^{-1/2}Nu_x$	$-Re_x^{-1/2}Sh_x$
0.0 0.1 0.2 0.3	0.3	0.02	0.5	0.2			15.076356 16.311422 17.828558 19.603687	0.531949 0.865588 1.23013 1.74362
0.3	0.0 0.1 0.2 0.3	0.02	0.5	0.2			3.971461 6.571446 9.401161 12.491079	0.818473 0.971720 1.138839 1.321664
0.3	0.30	0.02	0 0.5 1	0.2	2.183845 2.489511 2.818417	1.839443 1.828564 1.797756	3.872191 11.446637 19.716298	0.651987 2.099186 3.619574
0.3	0.30	0 0.01 0.02 0.03	0.5	0.2	1.289386 1.345371 1.401623 1.458222	1.087367 1.133068 1.179011 1.225273	9.077827 9.237560 9.401161 9.568735	1.107367 1.123087 1.138839 1.154612
0.3	0.3	0.02	0.5	0 0.2 0.4 0.6			56.750332 42.374143 33.583211 27.656099	10.83257 7.621294 5.822552 4.669863

5. Conclusion

A numerical solution has been presented for a rotating flow of Al_2O_3-Cu/water hybrid nanofluid over a stretchable sheet with thermal-diffusion and diffusion-thermo effects. The effects of Thermal radiation, Schmidt parameter, Suction, and volume fraction of Cu were considered for the flow study. Using MATLAB, a three-step finite-difference scheme called the Lobatto-IIIA was implemented to solve the governing non-linear ordinary differential equations.

The observations as a result of this study are:

(1) The primary velocity declines with rising values of the rotational parameter (ω).

(2) The temperature and concentration profile decline with an increase in the Dufour and Soret parameter values in the presence of suction.

(3) The temperature and concentration boundary layers increase with the rise in thermal radiation.

(4) The concentration profiles diminish with an increase in the values of the Schmidt parameter.

(5) The enhancement in the volume fraction of Copper (Cu) nanoparticles in Al_2O_3/water nanofluid leads to the decrease of the primary velocity and temperature profiles and a rise in the shape of transverse momentum and Concentration.

Nomenclature

u,v,w	x, y, z components of velocity (ms^{-1})	T_∞	Ambient temperature (K)
C_w	Free stream concentration	ρ	Fluid density (kgm^{-3})
λ	Stretching parameter	C_∞	Uniform constant concentration
T	The temperature of the fluid (K)	Ω	Angular velocity (ms^{-1})
D	Mass diffusivity coefficient	Rd	Radiation parameter
$\varphi 1, \varphi 2$	Nanoparticle's volume fraction	κ	Thermal conductivity (Wm^{-1}k^{-1})
C_p	Specific heat constant pressure (Jkgk^{-1})	ω	Angular velocity
C	The concentration of the species	S	Suction/injection
T_w	Surface temperature (K)	Re	Reynolds number
v	Kinematic viscosity (m^{2}s^{-1})	Sc	Schmidt number
Du	Dufour number	Sr	Soret number
Pr	Prandtl number	μ	Dynamic viscosity (kgm^{-1}s^{-1})
Subscript			
f	fluid	b_f	Base fluid
nf	Nano fluid	hnf	Hybrid nanofluid
$s1$	First solid particle	$s2$	Second solid particle
w	Condition at wall	∞	Ambient condition

Competing Interests

The authors declare that they have no competing interests.

Authors' Contributions

All the authors contributed significantly in writing this article. The authors read and approved the final manuscript.

References

[1] H. M. Ali, *Hybrid Nanofluids for Convection Heat Transfer*, Elsevier/Academic Press (2020), DOI: 10.1016/C2018-0-04602-2.

[2] H. M. Ali, H. Ali, H. Liaquat, H. T. B. Maqsood and M. A. Nadir, Experimental investigation of convective heat transfer augmentation for car radiator using ZnO–water nanofluids, *Energy* **84** (2015), 317 – 324, DOI: 10.1016/j.energy.2015.02.103.

[3] A. I. Alsabery, H. T. Kadhim, M. A. Ismael, I. Hashim and A. J. Chamkha, Impacts of amplitude and heat source on natural convection of hybrid nanofluids into a wavy enclosure via heatline approach, *Waves in Random and Complex Media* **33**(4) (2023), 1060 – 1084, DOI: 10.1080/17455030.2021.1896819.

[4] N. S. Anuar, N. Bachok and I. Pop, Radiative hybrid nanofluid flow past a rotating permeable stretching/shrinking sheet, *International Journal of Numerical Methods for Heat & Fluid Flow* **31**(3) (2020), 914 – 932, DOI: 10.1108/HFF-03-2020-0149.

[5] W. Arshad and H. M. Ali, Experimental investigation of heat transfer and pressure drop in a straight minichannel heat sink using TiO_2 nanofluid, *International Journal of Heat and Mass Transfer* **110** (2017), 248 – 256, DOI: 10.1016/j.ijheatmasstransfer.2017.03.032.

[6] M. Ataei, F. S. Moghanlou, S. Noorzadeh, M. Vajdi and M. S. Asl, Heat transfer and flow characteristics of hybrid Al_2O_3/TiO_2–water nanofluid in a minichannel heat sink, *Heat and Mass Transfer* **56** (2020), 2757 – 2767, DOI: 10.1007/s00231-020-02896-9.

[7] A. Aziz, T. Muhammad, A. Alsaedi and T. Hayat, An optimal study for 3D rotating flow of Oldroyd-B nanofluid with convectively heated surface, *Journal of the Brazilian Society of Mechanical Sciences and Engineering* **41** (2019), Article number: 236, DOI: 10.1007/s40430-019-1733-8.

[8] N. Bachok, A. Ishak and I. Pop, Boundary layer stagnation-point flow and heat transfer over an exponentially stretching/shrinking sheet in a nanofluid, *International Journal of Heat and Mass Transfer* **55**(25–26) (2012), 8122 – 8128, DOI: 10.1016/j.ijheatmasstransfer.2012.08.051.

[9] J. Buongiorno, Convective transport in nanofluids, *ASME Journal of Heat and Mass Transfer* **128**(3) (2006), 240 – 250, DOI: 10.1115/1.2150834.

[10] S. U. S. Choi and J. A. Eastman, Enhancing thermal conductivity of fluids with nanoparticles, *ASME International Mechanical Engineering Congress & Exposition*, November 12-17, 1995, San Francisco, CA, URL: https://ecotert.com/pdf/196525_From_unt-edu.pdf.

[11] K. Ezhil, S. K. Thavada and S. B. Ramakrishna, MHD slip flow and heat transfer of Cu-Fe_3O_4/ethylene glycol-based hybrid nanofluid over a stretching surface, *Biointerface Research in Applied Chemistry* **11**(4) (2021), 11956 – 11968, DOI: 10.33263/BRIAC114.1195611968.

[12] B. Fallah, S. Dinarvand, M. E. Yazdi, M. N. Rostami and I. Pop, MHD flow and heat transfer of SiC–TiO_2/DO hybrid nanofluid due to a permeable spinning disk by a novel algorithm, *Journal of Applied and Computational Mechanics* **5**(5) (2019), 976 – 988, DOI: 10.22055/JACM.2019.27997.1449.

[13] M. Ghalambaz, M. Sabour, I. Pop and D. Wen, Free convection heat transfer of MgO-MWCNTs/EG hybrid nanofluid in a porous complex shaped cavity with MHD and thermal radiation effects, *International Journal of Numerical Methods for Heat & Fluid Flow* **29**(11) (2019), 4349 – 4376, DOI: 10.1108/HFF-04-2019-0339.

[14] B. J. Gireesha, G. Sowmya, M. I. Khan and H. F. Öztop, Flow of hybrid nanofluid across a permeable longitudinal moving fin along with thermal radiation and natural convection, *Computer Methods and Programs in Biomedicine* **185** (2020), 105166, DOI: 10.1016/j.cmpb.2019.105166.

[15] T. Gul, M. Bilal, M. Shuaib, S. Mukhtar and P. Thounthong, Thin film flow of the water-based carbon nanotubes hybrid nanofluid under the magnetic effects, *Heat Transfer* **49**(6) (2020), 3211 – 3227, DOI: 10.1002/HTJ.21770.

[16] T. Hayat, A. Aziz, T. Muhammad, A. Alsaedi and M. Mustafa, On magnetohydrodynamic flow of second grade nanofluid over a convectively heated nonlinear stretching surface, *Advanced Powder Technology* **27**(5) (2016), 1992 – 2004, DOI: 10.1016/J.APT.2016.07.002.

[17] T. Hayat, T. Nasir, M. I. Khan and A. Alsaedi, Non-Darcy flow of water-based single (SWCNTs) and multiple (MWCNTs) walls carbon nanotubes with multiple slip conditions due to rotating disk, *Results in Physics* **9** (2018), 390 – 399, DOI: 10.1016/j.rinp.2018.02.044.

[18] W. Jamshed, S. R. Mishra, P. K. Pattnaik, K. S. Nisar, S. S. U. Devi, M. Prakash, F. Shahzad, M. Hussain and V. Vijayakumar, Features of entropy optimization on viscous second grade nanofluid streamed with thermal radiation: A Tiwari and Das model, Case Studies in *Thermal Engineering* **27** (2021), 101291, DOI: 10.1016/J.CSITE.2021.101291.

[19] A. U. Khan, S. Saleem, S. Nadeem and A. A. Alderremy, Analysis of unsteady non-axisymmetric Homann stagnation point flow of nanofluid and possible existence of multiple solutions, *Physica A: Statistical Mechanics and its Applications* **554** (2020), 123920, DOI: 10.1016/j.physa.2019.123920.

[20] M. Khan, T. Salahuddin, M. M. Yousaf, F. Khan and A. Hussain, Variable diffusion and conductivity change in 3D rotating Williamson fluid flow along with magnetic field and activation energy, *International Journal of Numerical Methods for Heat & Fluid Flow* **30**(5) (2020), 2467 – 2484, DOI: 10.1108/HFF-02-2019-0145.

[21] K. G. Kumar, G. K. Ramesh, S. A. Shehzad and F. M. Abbasi, Three-dimensional (3D) rotating flow of selenium nanoparticles past an exponentially stretchable surface due to solar energy radiation, *Journal of Nanofluids* **8**(5) (2019), 1034 – 1040, DOI: 10.1166/jon.2019.1662.

[22] K. G. Kumar, M. G. Reddy, P. V. Kumari, A. Aldalbahi, M. Rahimi-Gorji and M. Rahaman, Application of different hybrid nanofluids in convective heat transport of Carreau fluid, *Chaos, Solitons & Fractals* **141** (2020), 110350, DOI: 10.1016/j.chaos.2020.110350.

[23] K. G. Kumar, M. G. Reddy, S. A. Shehzad and F. M. Abbasi, A least square study on flow and radiative heat transfer of a hybrid nanofluid in a moving frame by considering a spherically-shaped particle, *Revista Mexicana de Física* **66**(2), 162 – 170, DOI: 10.31349/RevMexFis.66.162.

[24] B. A. Kuttan, S. Manjunatha and S. Jayanthi, Performance of four different nanoparticles in boundary layer flow over a stretching sheet in porous medium driven by buoyancy force, *International Journal of Applied Mechanics and Engineering* **25**(2) (2020), 1 – 10, DOI: 10.2478/ijame-2020-0016.

[25] L. A. Lund, Z. Omar, S. Dero, D. Baleanu and I. Khan, Rotating 3D flow of hybrid nanofluid on exponentially shrinking sheet: Symmetrical solution and duality, *Symmetry* **12**(10) (2020), 1637, DOI: 10.3390/sym12101637.

[26] F. Mabood and A. T. Akinshilo, Stability analysis and heat transfer of hybrid Cu-Al_2O_3/H_2O nanofluids transport over a stretching surface, *International Communications in Heat and Mass Transfer* **123** (2021), 105215, DOI: 10.1016/j.icheatmasstransfer.2021.105215.

[27] O. D. Makinde, F. Mabood and M. S. Ibrahim, Chemically reacting on MHD boundary-layer flow of nanofluids over a non-linear stretching sheet with heat source/sink and thermal radiation, *Thermal Science* **22**(1) (2018) (Part B), 495 – 506, DOI: 10.2298/TSCI151003284M.

[28] S. A. M. Mehryan, F. M. Kashkooli, M. Ghalambaz and A. J. Chamkha, Free convection of hybrid Al_2O_3-Cu water nanofluid in a differentially heated porous cavity, *Advanced Powder Technology* **28**(9) (2017), 2295 – 2305, DOI: 10.1016/j.apt.2017.06.011.

[29] M. Mustafa, T. Hayat and A. Alsaedi, Rotating flow of Oldroyd-B fluid over stretchable surface with Cattaneo-Christov heat flux: Analytic solutions, *International Journal of Numerical Methods for Heat & Fluid Flow* **27**(10) (2017), 2207 – 2222, DOI: 10.1108/HFF-08-2016-0323.

[30] M. K. Nayak, S. Shaw, V. S. Pandey and A. J. Chamkha, Combined effects of slip and convective boundary condition on MHD 3D stretched flow of nanofluid through porous media inspired by non-linear thermal radiation, *Indian Journal of Physics* **92** (2018), 1017 – 1028, DOI: 10.1007/s12648-018-1188-2.

[31] K. S. Nisar, U. Khan, A. Zaib, I. Khan and D. Baleanu, Exploration of aluminum and titanium alloys in the stream-wise and secondary flow directions comprising the significant impacts of magnetohydrodynamic and hybrid nanofluid, *Crystals* **10**(8) (2020), 679, DOI: 10.3390/cryst10080679.

[32] C. Ouyang, R. Akhtar, M. A. Z. Raja, M. T. Sabir, M. Awais and M. Shoaib, Numerical treatment with Lobatto IIIA technique for radiative flow of MHD hybrid nanofluid (Al_2O_3–Cu/H_2O) over a convectively heated stretchable rotating disk with velocity slip effects, *AIP Advances* **10** (2020), 055122, DOI: 10.1063/1.5143937.

[33] H. F. Oztop and E. Abu-Nada, Numerical study of natural convection in partially heated rectangular enclosures filled with nanofluids, *International Journal of Heat and Fluid Flow* **29**(5) (2008), 1326 – 1336, DOI: 10.1016/j.ijheatfluidflow.2008.04.009.

[34] A. Prathiba and V. L. Akavaram, Numerical investigation of a convective hybrid nanofluids around a rotating sheet, *Heat Transfer* **51**(4) (2022), 3353 – 3372, DOI: 10.1002/htj.22454.

[35] C. Ramreddy, P. V. S. N. Murthy, A. J. Chamkha and A. M. Rashad, Soret effect on mixed convection flow in a nanofluid under convective boundary condition, *International Journal of Heat and Mass Transfer* **64** (2013), 384 – 392, DOI: 10.1016/j.ijheatmasstransfer.2013.04.032.

[36] P. Rana, N. Srikantha, T. Muhammad and G. Gupta, Computational study of three-dimensional flow and heat transfer of 25 nm Cu–H_2O nanoliquid with convective thermal condition and radiative heat flux using modified Buongiorno model, *Case Studies in Thermal Engineering* **27** (2021), 101340, DOI: 10.1016/j.csite.2021.101340.

[37] G. Rasool, A. Shafiq and D. Baleanu, Consequences of Soret-Dufour effects, thermal radiation, and binary chemical reaction on Darcy Forchheimer flow of nanofluids, *Symmetry* **12**(9) (2020), 1421, DOI: 10.3390/SYM12091421.

[38] M. G. Reddy, M. V. V. N. L. Sudharani and K. G. Kumar, An analysis of dusty slip flow through a single-/multi-wall carbon nanotube, *Continuum Mechanics and Thermodynamics* **32** (2020), 971 – 985, DOI: 10.1007/s00161-019-00860-5.

[39] K. Sadiq, F. Jarad, I. Siddique and B. Ali, Soret and radiation effects on mixture of ethylene glycol-water (50%-50%) based maxwell nanofluid flow in an upright channel, *Complexity* **2021** (2021), Article ID 5927070, 12 pages, DOI: 10.1155/2021/5927070.

[40] M. R. Saffarian, M. Moravej and M. H. Doranehgard, Heat transfer enhancement in a flat plate solar collector with different flow path shapes using nanofluid, *Renewable Energy* **146** (2020), 2316 – 2329, DOI: 10.1016/j.renene.2019.08.081.

[41] H. Sardar, L. Ahmad, M. Khan and A. S. Alshomrani, Investigation of mixed convection flow of Carreau nanofluid over a wedge in the presence of Soret and Dufour effects, *International Journal of Heat and Mass Transfer* **137** (2019), 809 – 822, DOI: 10.1016/j.ijheatmasstransfer.2019.03.132.

[42] Z. Shah, E. Bonyah, S. Islam and T. Gul, Impact of thermal radiation on electrical MHD rotating flow of Carbon nanotubes over a stretching sheet, *AIP Advances* **9** (2019), 015115, DOI: 10.1063/1.5048078.

[43] N. A. Shah, I. L. Animasaun, J. D. Chung, A. Wakif, F I. Alao and C. S. K. Raju, Significance of nanoparticle's radius, heat flux due to concentration gradient, and mass flux due to temperature gradient: The case of Water conveying copper nanoparticles, *Scientific Reports* **11** (2021), Article number: 1882, DOI: 10.1038/s41598-021-81417-y.

[44] N. Shaheen, M. Ramzan, A. Alshehri, Z. Shah and P. Kumam, Soret-Dufour impact on a three-dimensional Casson nanofluid flow with dust particles and variable characteristics in a permeable media, *Scientific Reports* **11** (2021), Article number: 14513, DOI: 10.1038/s41598-021-93797-2.

[45] S. A. Shehzad, M. G. Reddy, P. Vijayakumari and I. Tlili, Behavior of ferromagnetic Fe_2SO_4 and titanium alloy Ti_6Al_4v nanoparticles in micropolar fluid flow, *International Communications in Heat and Mass Transfer* **117** (2020), 104769, DOI: 10.1016/j.icheatmasstransfer.2020.104769.

[46] M. Shoaib, M. A. Z. Raja, M. T. Sabir, M. Awais, S. Islam, Z. Shah and P. Kumam, Numerical analysis of 3-D MHD hybrid nanofluid over a rotational disk in presence of thermal radiation with Joule heating and viscous dissipation effects using Lobatto IIIA technique, *Alexandria Engineering Journal* **60**(4) (2021), 3605 – 3619, DOI: 10.1016/j.aej.2021.02.015.

[47] A. Shojaei, A. J. Amiri, S. S. Ardahaie, K. Hosseinzadeh and D. D. Ganji, Hydrothermal analysis of Non-Newtonian second grade fluid flow on radiative stretching cylinder with Soret and Dufour effects, *Case Studies in Thermal Engineering* **13** (2019), 100384, DOI: 10.1016/J.CSITE.2018.100384.

[48] M. Turkyilmazoglu, Effects of uniform radial electric field on the MHD heat and fluid flow due to a rotating disk, *International Journal of Engineering Science* **51** (2012), 233 – 240, DOI: 10.1016/j.ijengsci.2011.09.011.

[49] I. Uddin, R. Akhtar, Z. Zhiyu, S. Islam, M. Shoaib and M. A. Z. Raja, Numerical treatment for darcy-forchheimer flow of sisko nanomaterial with nonlinear thermal radiation by Lobatto IIIA technique, *Mathematical Problems in Engineering* **2019** (2019), Article ID 8974572, 15 pages, DOI: 10.1155/2019/8974572.

[50] I. Waini, A. Ishak and I. Pop, Dufour and Soret effects on Al_2O_3-water nanofluid flow over a moving thin needle: Tiwari and Das model, *International Journal of Numerical Methods for Heat & Fluid Flow* **31**(3) (2021), 766 – 782, DOI: 10.1108/HFF-03-2020-0177.

[51] C. Y. Wang, Stretching a surface in a rotating fluid, *Zeitschrift für angewandte Mathematik und Physik ZAMP* **39**(2) (1988), 177 – 185, DOI: 10.1007/BF00945764.

[52] H. Waqas, U. Farooq, M. Alghamdi, T. Muhammad and A. S. Alshomrani, On the magnetized 3D flow of hybrid nanofluids utilizing nonlinear radiative heat transfer, *Physica Scripta* **96**(9) (2021), 95202, DOI: 10.1088/1402-4896/ac0272.